Journal of The Electrochemical Society, **157** (7) G166-G169 (2010)
0013-4651/2010/157(7)/G166/4/$28.00 © The Electrochemical Society

Ti-Induced Recovery Phenomenon of Resistive Switching in ZrO_2 Thin Films

Dai-Ying Lee, Sheng-Yu Wang, and Tseung-Yuen Tseng[z]

Department of Electronics Engineering and Institute of Electronics, National Chiao Tung University, Hsinchu 300, Taiwan

In this study, we used W-probe directly contacted with the as-deposited ZrO_2 films to perform the resistive switching (RS) phenomenon, and the ZrO_2-based device finally came to break down (defined as BD-ZrO_2/Pt device). A remarkable phenomenon called "recovery" was observed, where the RS phenomenon appeared again in a broken ZrO_2-based device after Ti top electrode deposition. On the contrary, there was no such phenomenon while the Pt and Al top electrodes were deposited on the BD-ZrO_2/Pt devices. The Ti-induced recovery phenomenon of RS could be explained by the effects of the interface layer formation. The interface layers, TiO_z and ZrO_y, served as the oxygen reservoir and the series resistance, respectively, to provide sufficient oxygen ions for inducing the redox reaction of the conducting filament near the ZrO_y layer. Moreover, it also interpreted the high yield of the Ti/ZrO_2/Pt device. Therefore, the interface engineering of the resistive random access memory device is found very crucial to improve its performance for future commercial applications.
© 2010 The Electrochemical Society. [DOI: 10.1149/1.3428462] All rights reserved.

Manuscript submitted December 28, 2009; revised manuscript received March 22, 2010. Published May 14, 2010.

Recently, the electric-field induced resistive switching (RS) phenomenon has attracted great interest for potential memory applications known as resistive random access memory (RRAM). RRAM is one of the promising candidates due to its excellent properties including simple cell structure, small die size, long retention time, high operation speed, low power consumption, and easy process integration.[1-3] However, the RS mechanism and the corresponding regions where the RS phenomenon takes place are still unclear. Many measurement techniques,[4,5] theoretical simulations,[6,7] material analyses,[8,9] and even material and electrode combinations[10-13] are introduced to investigate the RS mechanism. Sawa et al. proposed that a Schottky barrier, the origin of the nonlinearity of the current–voltage (*I-V*) curve, was formed by a p-type semiconductor $Pr_{0.7}Ca_{0.3}MnO_3$ and a low work function metal with strong oxygen-gettering ability, and the resultant RS mechanism based on Schottky barrier modulation was suggested.[10] Moreover, the interface reaction and interdiffusion between electrodes and RS matrixes led to an oxygen-depleted interface and resulted in space-charge-limited conduction (SCLC).[5,14,15] Even both aforementioned mechanisms were important to explaining the interfacial RS phenomenon.[16] On the contrary, Beck et al. reported that the charge transfer within the bulk film dominated the RS behavior.[17]

The most possible and popular RS mechanism, however, was believed to be the formation/rupture of the conducting filament, where the conducting filament was formed in the localized high electrical field region and the high conductive state (on state) was achieved.[9] The conducting filament was then ruptured due to the reoxidization induced by local Joule heating near the anode to switch back into the low conducting state (off state).[4] Kim et al. further concluded that the formation/rupture of the conducting filament took place in the localized region (3–10 nm thick) near the anode.[18] In addition, Inoue et al. proposed a "faucet model" that the "electric faucet" switched off and on at the high resistive interface to control the homogeneous and inhomogeneous transition of the current distribution, respectively.[19] However, it was also possible that the rupture occurred in the middle of the conducting filament, where the produced temperature was the highest by Joule heating.[8]

As for the ZrO_2-based RS memories, Lee et al. first explained that the RS mechanism was dominated by band bending, where it is controlled by electron trapping and detrapping at the Zr^+ trap in the ZrO_2 layer.[20] However, Wu et al. believed that the reaction between the Al electrode and O^{2-} ions in the ZrO_2 films led to the formation/rupture of the local conducting filament.[21] In our previous papers, the ZrO_2-based devices with a Ti top electrode were demonstrated to exhibit better RS characteristics than those with Al and Pt top electrodes, and a transition from nonpolar to bipolar RS was also observed. Ti top electrode was an oxygen-gettering material and easily extracted a large amount of oxygen ions from ZrO_2 films, further causing the formation of the interface. This result was characterized and confirmed by both high resolution transmission electron microscopy and secondary ions mass spectrometry analyses. Hence, an RS mechanism was proposed wherein the region where filament formation/rupture occurred would be confined near the interface between Ti and ZrO_2.[12-14,22]

In this study, we observe a remarkable phenomenon called "recovery," where the RS phenomenon appeared again in a broken ZrO_2-based device after depositing Ti top electrode. This recovery phenomenon is attributed to the formation of an interface layer, which has a profound influence on the RS properties and device yield. The demonstrated recovery phenomenon in this study gives an insight into RS mechanism and improvement in RRAM performance.

Experimental

ZrO_2 films (50 nm thick) were deposited on Pt/Ti/SiO_2/Si substrates at 250°C by radio-frequency magnetron sputtering, where the deposition pressure was maintained at 10 mTorr with a gas mixture of oxygen and argon at a mixing ratio of 6:12. Top electrodes, Al, Pt, and Ti were deposited by using thermal or electron-beam evaporation at ambient temperature with a diameter of 250 μm patterned by the shadow mask process. There is no high temperature annealing process performed after depositing top electrodes. The thicknesses of Al, Ti, and Pt top electrodes were 300, 150, and 80 nm, respectively. An Agilent 4155C semiconductor parameter analyzer was used to measure the electrical characteristics of the ZrO_2-based memory device in ambient atmosphere at room temperature.

Results and Discussion

To clarify the Ti-induced recovery phenomenon of RS in ZrO_2 films, we perform the following procedures. First, a shadow mask is fixed on the surface of the as-deposited ZrO_2 films, as shown in Fig. 1a. The Pt bottom electrode is common, and the W-probe is directly contacted with the unmasked region where the top electrode is to be formed (defined as the W-probe/ZrO_2/Pt device). Figure 1b shows the bias-independent RS behavior performed in the W-probe/ZrO_2/Pt (black line), where an 8 V forming voltage with a 5 mA current compliance is required before performing any RS (not shown here). The forming process is the common effect reported in RRAM-related literatures, which is similar to a soft dielectric breakdown, and the conducting filament is thus developed.[4] Due to the large initial resistance and the forming process in W-probe/ZrO_2/Pt, the ZrO_2 film is not pierced through by the W-probe. However, for

[z] E-mail: tseng@cc.nctu.edu.tw

Downloaded on 2016-09-15 to IP 130.203.136.75 address. Redistribution subject to ECS terms of use (see ecsdl.org/site/terms_use) unless CC License in place (see abstract).

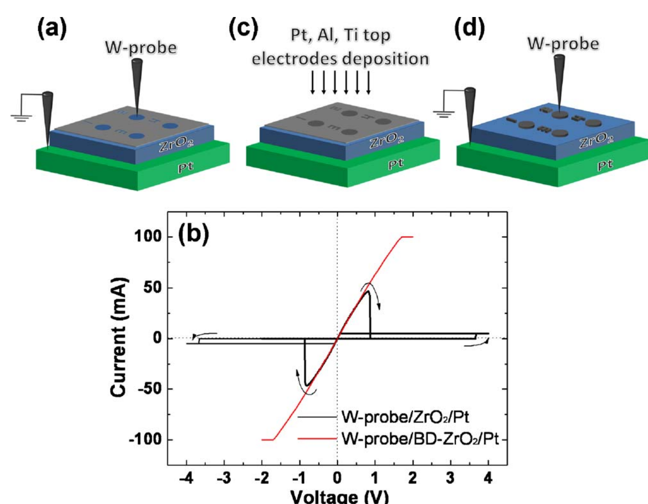

Figure 1. (Color online) (a) W-probe is directly contacted with the unmasked region with Pt bottom electrode common. (b) The nonpolar RS behavior in W-probe/ZrO_2/Pt (black line), and after several ten successive RS cycles, the ZrO_2-based device cannot be further switched back into the off state (red line). (c) The deposition of the Pt, Al, and Ti top electrodes. (d) The *I-V* characteristics are performed for the ZrO_2-based devices after stacking various top electrodes.

the lower yield (about 17%) of the W-probe/ZrO_2/Pt device, the W-probe might possibly pierce into the ZrO_2 film to some degree to lower the device yield. Furthermore, the poor contact between the W-probe and the ZrO_2 film might also decrease the device yield. Based on our previous experimental results,[12-14] the formation and rupture of the conducting filament are suggested to dominate the RS property in the W-probe/ZrO_2/Pt device. After operating several ten successive RS cycles, the W-probe/ZrO_2/Pt device cannot be further switched into the off state and the device breaks down (defined as the BD-ZrO_2/Pt device and the *I-V* curve, as shown in the red line in Fig. 1b). The RS property disappears due to the formation of the very strong conducting filament within the ZrO_2 film, and a higher current might be needed to produce sufficient Joule heat to rupture the conducting filament during the off process. However, the maximum limitation of the current compliance in Agilent 4155C is 100 mA.

To examine the influence of top electrode materials on the RS behavior of BD-ZrO_2/Pt devices, the Pt, Al, and Ti top electrodes are deposited on regions of the BD-ZrO_2/Pt devices, respectively, where the mask is uncovered, as shown in Fig. 1c. Consequentially, the electrical measurements of Pt/BD-ZrO_2/Pt, Al/BD-ZrO_2/Pt, and Ti/BD-ZrO_2/Pt devices are implemented, respectively (Fig. 1d). Figure 2a depicts the *I-V* properties before (red line) and after (black line with empty circle symbol) deposition of the Pt top electrode, where the arrows and the marked number indicate the voltage sweeping direction and sequence, respectively. It indicates that the Pt/BD-ZrO_2/Pt device remains in the on state with negligible resistance change and no further RS phenomenon is observed by applying neither positive nor negative bias on them. However, after deposition of the Al top electrode, initially, there is a little difference at low bias voltage (below 0.5 V) between the W-probe/BD-ZrO_2/Pt (red line) and Al/BD-ZrO_2/Pt (blue line with empty circle symbol) devices, as shown in Fig. 2b. Therefore, a thin interface layer is expected to be induced between the Al top electrode and the BD-ZrO_2 film and is believed to cause this small resistance difference (marked as 1 in Fig. 2b). While applying higher voltage on the Al/BD-ZrO_2/Pt device, this interface layer is so thin that it is easily destroyed, and the resistance produced by the interface layer is reduced (marked as 2 in Fig. 2b). No reproducible RS phenomenon is presented in this device either.

We have characterized the formation of the interface layers between the Ti top electrode and the as-deposited ZrO_2 film in our previous study.[13] As for the Ti/BD-ZrO_2/Pt device in this experiment, it shows an originally distinct difference in *I-V* curves as compared with the Pt/BD-ZrO_2/Pt and Al/BD-ZrO_2/Pt devices. The initial resistance of the Ti/BD-ZrO_2/Pt device is relatively large and ~2 to 2.5 kΩ, as indicated in Fig. 3a (marked as 1). Therefore, the interface layer formed between Ti and BD-ZrO_2 is also concluded in this study. What is more important is that the RS phenomenon appears again in the BD-ZrO_2/Pt device after stacking the Ti top electrode. A remarkable phenomenon called recovery of RS is discovered and the RS property is also reproducible in the Ti/BD-ZrO_2/Pt device, as shown in Fig. 3a. In addition, the as-deposited ZrO_2 devices (not directly measured by the W-probe) using Ti top electrode show higher device yield than those with Pt and Al top electrodes, as shown in Fig. 4. As a result, the formed interface layer is proven to significantly influence and determine the RS characteristics even if the memory devices break down at first.

Such an interface layer is also investigated to modify ohmic conduction in the W-probe/BD-ZrO_2/Pt device after Ti electrode deposition. The curve fitting performed for both positive and negative bias regions of the initial *I-V* characteristics in the Ti/BD-ZrO_2/Pt device and the double-logarithmic plots are shown in Fig. 3b and c, respectively. The conduction mechanism in the Ti/BD-ZrO_2/Pt device agrees well with the SCLC theory. In the low voltage positive bias region, ohmic conduction (slope = 1) is assumed to be caused by the thermal-free carriers exceeding the injected ones, which is followed by the trap-unfilled SCLC (slope = 2). Then, due to the conducting filament formation and trapping the injected charges, an abrupt current increase appears. The second I-V^2 characteristics are observed again in the positive bias region due to trapping centers occupied by the injected carrier, creating a space charge near the electrode and resulting in an electric field to restrict further carrier injection (trap-filled SCLC). Finally, the on state is achieved and obeys the ohmic conduction in the voltage-decreasing scan, as shown in Fig. 3b. Figure 3c depicts the off process in the negative bias region, and the similar conduction mechanism is observed, which obeys the SCLC theory with rupturing the conducting fila-

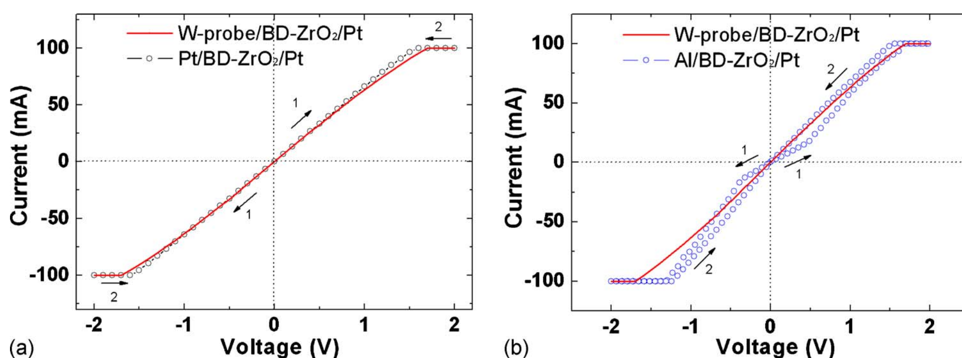

Figure 2. (Color online) The *I-V* properties of the BD-ZrO_2/Pt device before (red line) and after (line with empty circle symbol) stacking (a) Pt and (b) Al top electrodes. The arrows and the marked number indicate the sweeping direction and the sweeping sequence, respectively.

Downloaded on 2016-09-15 to IP 130.203.136.75 address. Redistribution subject to ECS terms of use (see ecsdl.org/site/terms_use) unless CC License in place (see abstract).

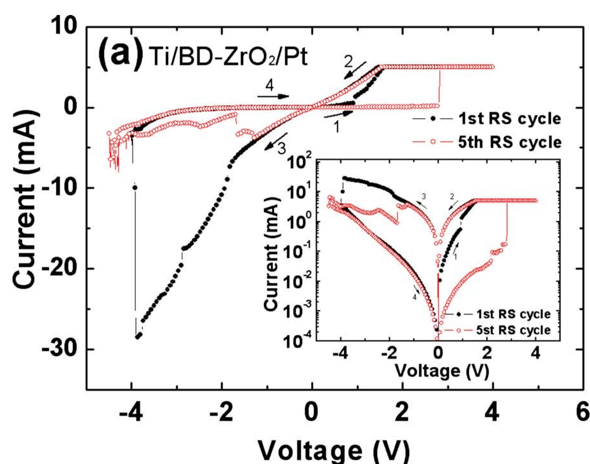

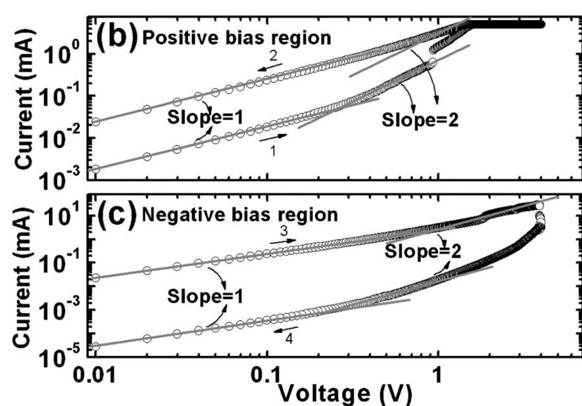

Figure 3. (Color online) (a) The Ti-induced recovery phenomenon of RS in the BD-ZrO_2/Pt device after fabricating Ti top electrode. The first and fifth RS cycles are shown, demonstrating the bipolar RS characteristics. *I-V* curves in (b) positive and (c) negative bias regions in the Ti/BD-ZrO_2/Pt device in double-logarithmic plot.

ment. Therefore, the Ti/BD-ZrO_2/Pt device exhibits the same carrier conduction behavior as that in the activated Ti/ZrO_2/Pt device in our previous paper.[14]

The Ti-induced recovery phenomenon of RS can be schematically elucidated in Fig. 5. After the forming process and performing several ten RS cycles by direct W-probe contact, plenty of possible point defects such as oxygen vacancies, zirconium interstitial, e^-, and h^+ are expected to be formed and coalescent within the ZrO_2

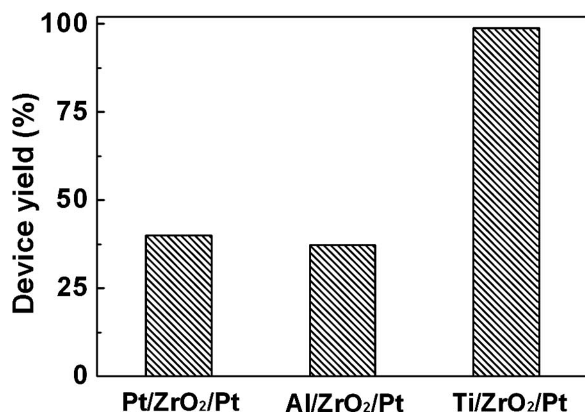

Figure 4. Diagram of device yield for Pt/ZrO_2/Pt, Al/ZrO_2/Pt, and Ti/ZrO_2/Pt devices.

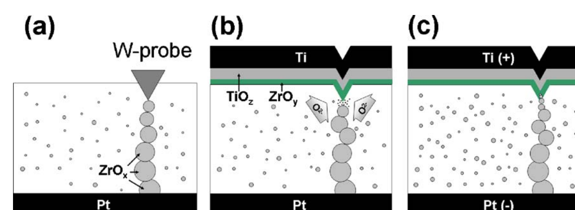

Figure 5. (Color online) Schematic diagrams of (a) the strong conducting filament formed in the W-probe/BD-ZrO_2/Pt device after successive RS cycles. (b) The TiO_z and ZrO_y interface layers, induced by stacking Ti top electrode, cause the intermediate state between on and off states. (c) The formed conducting filament penetrates through the ZrO_y interface layer when being switched into on state.

film. The conducting filament is considered to consist of these point defects, especially oxygen vacancy. The detailed mechanisms of nonpolar and bipolar RS in the ZrO_2-based device have been reported in our previous studies.[13,14,22] Eventually, the W-probe/ZrO_2/Pt device breaks down and always remains in the on state, which could be due to the formation of the very strong conducting filament composed of ZrO_x ($x < 2$) clusters, as shown in Fig. 5a. After fabricating the Ti top electrode on the surface of BD-ZrO_2/Pt, the resultant Ti/BD-ZrO_2/Pt device initially shows a higher resistance value than that in the W-probe/BD-ZrO_2/Pt device.

Oxygen diffusion within the ZrO_2 bulk crystal is typically transported through oxygen vacancies. In addition, grain boundary diffusion is significant in the fine-grained polycrystalline metal oxides. Oxygen diffusion along such paths is also possible in thin amorphous films, such as our ZrO_2 films in this study, although the experimental results obtained so far do not allow us to quantify the relative contributions of the oxygen transport mechanisms. An oxygen diffusivity across metal oxide films of the order 10^{-16} cm^2/s can be estimated for our ZrO_2 films at 300 K.[23] For an oxygen diffusion length of 5 nm, the required diffusion time is ~10 min, which is much less than the duration of our Ti deposition process (over 200 min). Because Ti top electrode is a strong oxygen-gettering material and easily extracts a large amount of oxygen ions from the ZrO_2 film, the oxygen ion migration from the ZrO_2 film to the Ti top electrode possibly happens even at room temperature. Therefore, the oxygen-deficient ZrO_2 layer (defined as ZrO_y layer, where $x < y < 2$) and the oxidized Ti layer (defined as TiO_z, where $z \ll 2$) are believed to be formed.

The conductive TiO_z layer here is proposed to be employed as an oxygen reservoir.[13,14] During the above process of the interface layer formation, as the oxygen ions migrate from the bulk ZrO_2 film across the ZrO_x clusters near the Ti/ZrO_2 interface, partial oxygen ions recombine with oxygen vacancies in the ZrO_x clusters. Hence, the incomplete rupture of the conducting filament near the Ti/ZrO_2 interface would be observed and is shown in Fig. 5b, which causes an intermediate resistance state between the on and off states indicated in Fig. 3a.

Sequentially, when applying positive voltage bias on Ti top electrode with a current compliance of 5 mA on the Ti/BD-ZrO_2/Pt device, the device is switched into the on state. The oxygen ions and electrons that originally exhibit in the incomplete ruptured conducting filament are extracted and then migrate across the ZrO_y layer toward the oxygen reservoir, the TiO_z layer, while the oxygen vacancies move from the interface toward the Pt bottom electrode (Fig. 5c). Moreover, due to the exhibition of slope = 2 in the on state as depicted in Fig. 3b, the conducting filament is thought to be formed again and in series with interface layers (TiO_z and ZrO_y) between Ti and Pt electrodes (Fig. 5c). Further changing the bias polarity into the negative voltage causes oxygen ions to migrate from the TiO_z layer to annihilate the oxygen vacancies in the ZrO_x clusters by the assistance of Joule heating. Because the ZrO_y layer is

Downloaded on 2016-09-15 to IP 130.203.136.75 address. Redistribution subject to ECS terms of use (see ecsdl.org/site/terms_use) unless CC License in place (see abstract).

more resistive than the TiO_z layer and the ZrO_x clusters, most Joule heating is expected to be produced around the ZrO_y layer. The location where the conducting filament is completely ruptured is elucidated near or within the ZrO_y layer. Therefore, the Ti-induced recovery phenomenon of RS can be explained by how the formation of the oxygen reservoir TiO_z layer accompanies the ZrO_y layer to provide sufficient oxygen ions for inducing the redox reaction of the ZrO_x clusters in the conducting filament.

The interdiffusion between the Al top electrode and ZrO_2 film is also expected to occur but forms thinner oxygen-deficient ZrO_2 layer and thinner oxidized Al layer, which is deduced from the small resistance difference marked as 1 in Fig. 2b before and after depositing the Al electrode. However, the thin interfaces induced by Al cannot sustain the voltage drop when further RS operation is performed. As compared with Al top electrode, Ti top electrode, therefore, is suggested to exhibit relatively large ability for extracting and dissolving oxygen, which leads to why the Al top electrode is not effective to recover the RS behavior like the Ti top electrode. The similar result was reported by Kim et al., who have investigated the effects of Al and Ti electrodes on the ZrO_2/Si substrate interface, for future high-*k* dielectric ZrO_2 oxide in metal-oxide-semiconductor field effect transistor application.[23] Deposition of the ZrO_2 film on a Si substrate was often accompanied with a SiO_2-based interface layer (an unwanted low-*k* material) between the ZrO_2 and Si substrates due to oxidation of the Si surface. Such interface layer was eliminated by using an oxygen-gettering Ti overlayer on the ZrO_2 film. Oxygen ions from the interface migrated across the ZrO_2 dielectric layer and dissolved into the Ti overlayer near 300 K. However, the SiO_2-based interface layer was not eliminated by using Al as the overlayer. Although Al also extracted oxygen ions from the ZrO_2 dielectric layer, only a very thin interface between the Al and ZrO_2 dielectric layer was formed. In addition, such thin interface was excepted because the oxidized Al at the interface further restricted the oxygen diffusion into the Al electrode.[24] As a result, Ti electrode is considered to exhibit relatively large ability for extracting and dissolving oxygen than Al electrode.

The functions of the TiO_z and ZrO_y layers also manifest the high yield of the Ti/ZrO_2/Pt device, as indicated in Fig. 4. The TiO_z layer can easily provide more sufficient oxygen ions than the ZrO_2 matrix, and the possibility for Joule heating to occur near the resistive ZrO_y layer is higher.[14] As for both Pt/ZrO_2/Pt and Al/ZrO_2/Pt devices, there is no assistance from such interface layers. More energy, therefore, is necessary to drive the oxygen ions from the ZrO_2 matrix to cause the formation/rupture region of the filament. The more energy is required, the higher possibility the RS fails to be performed. It is the reason why the Ti/ZrO_2/Pt devices exhibit higher yield than the Pt/ZrO_2/Pt and Al/ZrO_2/Pt devices. As a result, the properties of the interface layers would be the critical factor in determining RRAM performance and even its device yield.

Conclusion

In summary, the influence of the Pt, Al, and Ti top electrodes on the switching behavior of BD-ZrO_2/Pt devices is compared. Based on the *I-V* curves of Pt/BD-ZrO_2/Pt devices, the interface layer within Pt/BD-ZrO_2 can be neglected, but the Al top electrode causes a very thin interface layer on the BD-ZrO_2 layer. As for the Ti/BD-ZrO_2/Pt device, the TiO_z and ZrO_y interface layers are expected to be formed due to the oxygen-gettering ability of Ti, leading to a very different *I-V* curve, as compared with the two aforementioned devices. The TiO_z layer is proposed to be employed as an oxygen reservoir, which provides oxygen ions for the redox reaction of the ZrO_x clusters in the conducting filament. Furthermore, the major Joule heating is produced around the ZrO_y layer, and the rupture of the conducting filament, therefore, is assumed to be confined within/near the ZrO_y layer. A notable Ti-induced recovery phenomenon of RS in the ZrO_2 film is introduced and the high yield of the Ti/ZrO_2/Pt device is revealed as well. Consequentially, the interface engineering of the RRAM cell is very important to improve its performance for realizing future commercial applications.

Acknowledgment

This work was supported by the National Science Council, Taiwan under project NSC 96-2628-E-009-166-MY3.

National Chiao Tung University assisted in meeting the publication costs of this article.

References

1. G. Baek, M. S. Lee, S. Seo, M. J. Lee, D. H. Seo, D.-S. Suh, J. C. Park, S. O. Park, H. S. Kim, I. K. Yoo, et al., *Tech. Dig. - Int. Electron Devices Meet.*, **2004**, 587.
2. M. J. Lee, Y. Park, B. S. Kang, S. E. Ahn, C. Lee, K. Kim, W. Xianyu, G. Stefanovich, J. H. Lee, S. J. Chung, et al., *Tech. Dig. - Int. Electron Devices Meet.*, **2007**, 771.
3. H. Y. Lee, P. S. Chen, T. Y. Wu, Y. S. Chen, C. C. Wang, P. J. Tzeng, C. H. Lin, F. Chen, C. H. Lien, and M. J. Tsai, *Tech. Dig. - Int. Electron Devices Meet.*, **2008**, 297.
4. K. Kinoshita, T. Tamura, M. Aoki, Y. Sugiyama, and H. Tanaka, *Appl. Phys. Lett.*, **89**, 103509 (2006).
5. S. Tsui, A. Baikalov, J. Cmaidalka, Y. Y. Sun, Y. Q. Wang, Y. Y. Xue, C. W. Chu, L. Chen, and A. J. Jacobson, *Appl. Phys. Lett.*, **85**, 317 (2004).
6. S. C. Chae, J. S. Lee, S. Kim, S. B. Lee, S. H. Chang, C. Liu, B. Kahng, H. Shin, D.-W. Kim, C. U. Jung, et al., *Adv. Mater.*, **20**, 1154 (2008).
7. U. Russo, D. Ielmini, C. Cagli, A. L. Lacaita, S. Spiga, C. Wiemer, M. Perego, and M. Fanciulli, *Tech. Dig. - Int. Electron Devices Meet.*, **2007**, 775.
8. M. Janousch, G. I. Meijer, U. Staub, B. Delley, S. F. Karg, and B. P. Andreasson, *Adv. Mater.*, **19**, 2232 (2007).
9. M. K. Yang, J. W. Park, T. K. Ko, and J. K. Lee, *Appl. Phys. Lett.*, **95**, 042105 (2009).
10. A. Sawa, T. Fujii, M. Kawasaki, and Y. Tokura, *Appl. Phys. Lett.*, **85**, 4073 (2004).
11. K. Tsubouchi, I. Ohkubo, H. Kumigashira, M. Oshima, Y. Matsumoto, K. Itaka, T. Ohnishi, M. Lippmaa, and H. Koinuma, *Adv. Mater.*, **19**, 1711 (2007).
12. C. Y. Lin, C. Y. Wu, C. Y. Wu, T. Y. Lee, F. L. Yang, C. Hu, and T. Y. Tseng, *IEEE Electron Device Lett.*, **28**, 366 (2007).
13. C. Y. Lin, C. Y. Wu, C. Y. Wu, T. Y. Tseng, and C. Hu, *J. Appl. Phys.*, **102**, 094101 (2007).
14. C. Y. Lin, S. Y. Wang, D. Y. Lee, and T. Y. Tseng, *J. Electrochem. Soc.*, **155**, H615 (2008).
15. Y. W. Xie, J. R. Sun, D. J. Wang, S. Liang, and B. G. Shen, *J. Appl. Phys.*, **100**, 033704 (2006).
16. T. Harada, I. Ohkubo, K. Tsubouchi, H. Kumigashira, T. Ohnishi, M. Lippmaa, Y. Matsumoto, H. Koinuma, and M. Oshima, *Appl. Phys. Lett.*, **92**, 222113 (2008).
17. A. Beck, J. G. Bednorz, Ch. Gerber, C. Rossel, and D. Widmer, *Appl. Phys. Lett.*, **77**, 139 (2000).
18. K. M. Kim, B. J. Choi, Y. C. Shin, S. Choi, and C. S. Hwang, *Appl. Phys. Lett.*, **91**, 012907 (2007).
19. I. H. Inoue, S. Yasuda, H. Akinaga, and H. Takagi, *Phys. Rev. B*, **77**, 035105 (2008).
20. D. Lee, H. Choi, H. Sim, D. Choi, H. Hwang, M. J. Lee, S. A. Seo, and I. K. Yoo, *IEEE Electron Device Lett.*, **26**, 719 (2005).
21. X. Wu, P. Zhou, J. Li, L. Y. Chen, H. B. Lv, Y. Y. Lin, and T. A. Tang, *Appl. Phys. Lett.*, **90**, 183507 (2007).
22. S. Y. Wang, D. Y. Lee, T. Y. Tseng, and C. Y. Lin, *Appl. Phys. Lett.*, **95**, 112904 (2009).
23. H. Kim, P. C. McIntyre, C. O. Chui, K. C. Saraswat, and S. Stemmer, *J. Appl. Phys.*, **96**, 3467 (2004).
24. W. W. Smeltzer, *J. Electrochem. Soc.*, **103**, 209 (1956).

Downloaded on 2016-09-15 to IP 130.203.136.75 address. Redistribution subject to ECS terms of use (see ecsdl.org/site/terms_use) unless CC License in place (see abstract).